Appl Phys B (2010) 99: 499–502
DOI 10.1007/s00340-010-3909-x

Applied Physics B
Lasers and Optics

Double negative in flexural single metal layer at visible frequencies

C. Hu · X. Chen · Q. Feng · X. Luo

Received: 1 September 2009 / Revised version: 15 December 2009 / Published online: 5 February 2010

Abstract We theoretically investigate a thin single metal layer covered on sub-wavelength dielectric grating. Numerical simulations show that the structure has negative index in the normal direction at visible frequencies. Structural investigation demonstrates that the simultaneous negative permittivity and permeability at an overlapping frequency range are attributed to the metal cut-wire and "U"-shaped structure disassembled from the structure, respectively. Furthermore, parametric exploration for practical fabrication is presented.

1 Introduction

Recently, simultaneous negative permeability (μ) and permittivity (ε) of a composite structure have attracted much attention due to their ability in achieving negative refractive index (n) meta-materials with low losses. However, the biggest challenge is the simultaneous realization of negative μ and ε at an overlapping frequency range. The split-ring structure proposed by Pendry et al. [1] and some analogous structures [2–7] have permitted one to modulate μ to be negative at a narrow range, while it is difficult to get negative ε at the same range when only these structures are considered [8]. Periodic continuous metal wire, which can be seen as a diluted Drude metal [9], can effectively push the effective plasmon frequency of the metal wire structure to below the bulk plasmon frequency of metal. In other words, periodic continuous metal wire can modulate ε to be negative and simultaneously obtain small $|\mathrm{Re}(\varepsilon)|$ to meet practical applications at the visible frequency range. Combining the two basic structures (split-ring and periodic continuous metal wire), both negative μ and ε can be obtained to produce negative n at the frequency range of interest [7, 10, 11]. Based on the design idea, several experimental verifications of negative n at microwave [12], infrared [13–15] and visible frequencies [16] have been demonstrated. In this paper, unlike the multi-layer designs proposed previously, a single-layer structure is theoretically investigated to demonstrate both negative μ and ε at an overlapping frequency range. Numerical simulations show that negative n with effective transmission (about 30%, averaged value) is obtained at visible frequency range.

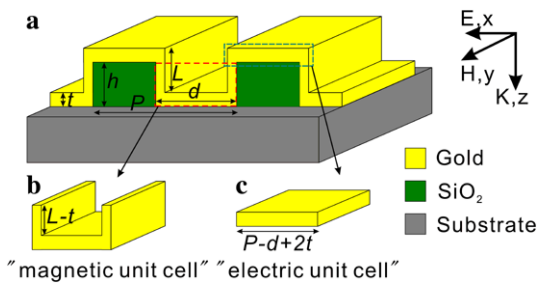

Fig. 1 Schematic drawing of S-ML design at visible frequencies (only two periods are shown). (**a**) S-ML, (**b**) "U"-shaped structure and (**c**) cut-wire disassembled from S-ML. The *right-up inset* shows the orientation of electromagnetic wave used in the simulation. The parameters of S-ML, P, h, d, t and L, are 260, 50, 140, 20, 50 nm, respectively

C. Hu · X. Chen · Q. Feng · X. Luo (✉)
State Key Laboratory of Optical Technologies for Microfabrication, Institute of Optics and Electronics, Chinese Academy of Sciences, P.O. Box 350, Chengdu 610209, China
e-mail: lxg@ioe.ac.cn
Fax: +86-28-85100210

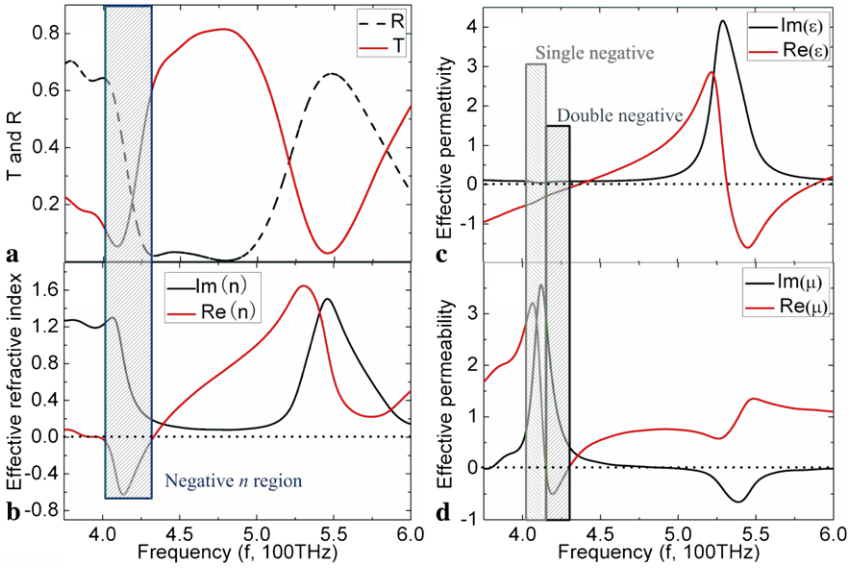

Fig. 2 Transmission and reflection spectra of S-ML (**a**). The retrieved n (**b**), ε (**c**) and μ (**d**)

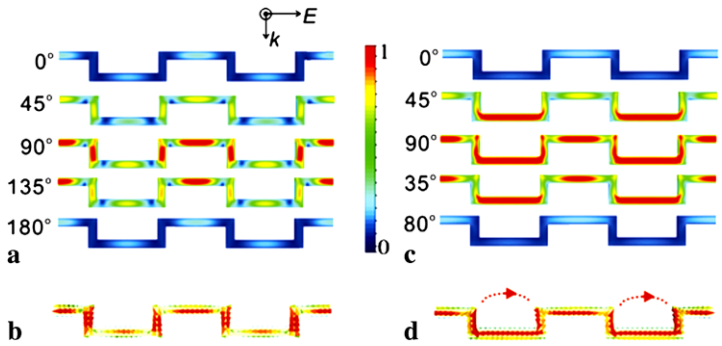

Fig. 3 Distributions of local current density at electric (**a**) and magnetic (**c**) resonance position. (**b**), (**d**): The current at 90° phase point corresponds to the electric and magnetic resonance, respectively. The *inset in (a)* shows the incident electromagnetic wave used in the simulation. All share the same color bar

2 Double negative design and results

Figure 1 demonstrates the design of the structure. A flexural single metal layer (S-ML) is covered on a pre-prepared one-dimensional dielectric grating to construct effective electric and magnetic resonators, which are the "U"-shaped structure and the cut-wire as shown in Fig. 1b and c, respectively. The two structures are utilized to support effective magnetic and electric responses. In simulation, a perfect Electric Boundary (PEC) is used to realize periodic arrangement in the x direction. Correspondingly, a Perfect Magnetic Boundary (PMC) is used to account for infinite in y direction. Computer simulation is carried out using the Finite-Difference Time-Domain (FDTD) method. The characteristic of gold at visible frequencies is described by the Drude model [17]. In this paper, the effective permittivity ($\varepsilon_{\text{gold}}$) of gold is $\varepsilon_{\text{gold}} = \varepsilon_0 - \omega_p^2/(\omega^2 + i\omega\gamma)$ in the visible range. The bulk plasmon resonance frequency $\omega_p = 1.4\text{e} + 16$ rad/s, and the collision frequency $\gamma = 1.1\text{e} + 14$ rad/s. The contribution of interband transitions can be approximated by a positive constant (ε_0) in gold's Drude model. For visible wavelengths, ε_0 is about 9.9 [18]. Using normal incident light with the electric polarization direction shown in Fig. 1, the spectra of S-ML and the retrieved electromagnetic parameters, including n, μ and ε [19, 20] are obtained as shown in Fig. 2. Obviously, two stop bands are observed at 410 and 540 THz in Fig. 2a. Corresponding to the first stop band, a negative n is obtained in the frequency range between 397 and 433 THz as shown in Fig. 2b.

3 Discussions

3.1 Resonance discussions

Resonance discussions are carried out to find out the underlying physical origin of the negative n of S-ML shown in Fig. 2b. Obviously, a strong oscillation of $\varepsilon(\mu)$ and a concomitant small anti-oscillation of $\mu(\varepsilon)$ are observed at 540 (410) THz in Fig. 2c (Fig. 2d). These characteristics, which are analogous with the discussions in Ref. [21], indicate the existence of electromagnetic resonances in S-ML.

A further investigation is the local current density distribution of the two resonances at 410 and 540 THz. Figure 3 demonstrates the simulated results at different phase points (0°, 45°, 90°, 135° and 180°). First, an oscillating current

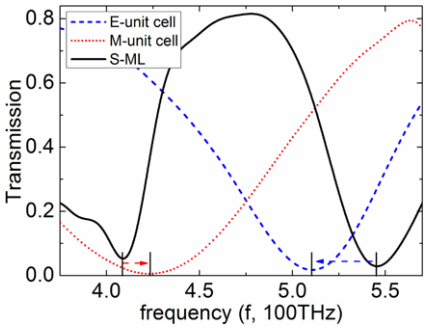

Fig. 4 Transmission spectra of S-ML (*black solid line*, marked by "S-ML"), periodic "U"-shaped structure (*red dot line*, marked by "M-unit cell") and periodic cut-wire (*blue dash line*, marked by "E-unit cell"). All three structures share the same period (P) shown in Fig. 1a, and the parameters of magnetic and electric unit cell are also shown in Fig. 1b and c respectively

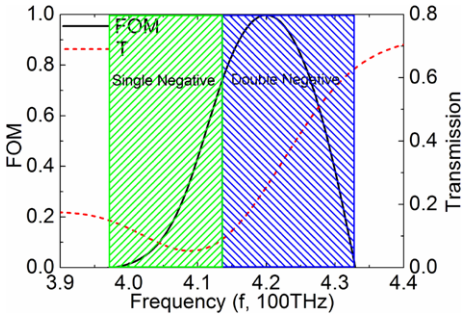

Fig. 5 FOM (*left, solid*) and respective transmission (*right, dash*) of S-ML in the region of negative n

in the cut-wire, located on the top/bottom of the dielectric grating, is found at 540 THz as shown in Fig. 3b. It means that the cut-wire can be seen as an electric oscillator at this frequency point. Second, a current "loop" is constructed in the "U"-shaped structure at 410 THz as shown in Fig. 3d. In the region of capacitance, conductive current is replaced by displacement current. It is a typical current distribution of magnetic response. So it can be concluded that the resonance at 540 (410) THz is an electric (magnetic) resonance supported by the cut-wire (the "U"-shaped) structure. This conclusion is consistent with the electric and magnetic oscillation shown in Fig. 2c and d.

3.2 Structural investigation

Following the resonance discussions above, it can be established that the simultaneous electric and magnetic resonance is attributed to the cut-wire and the "U"-shaped structure in S-ML, respectively. In this section, the individual response of the cut-wire and the "U"-shaped structure is investigated to understand their respective role in S-ML. Figure 4 shows the simulated results. The cut-wire, the "U"-shaped structure and S-ML are marked by "E-unit cell", "M-unit cell" and "S-ML", respectively. Obviously, the individual cut-wire and "U"-shaped structure have respective resonance near the two stop band of S-ML. Compared with the spectra of S-ML, the electric (magnetic) resonance shifts from 540 to 510 THz (from 410 to 425 THz). These shifts can be understood as follows.

First, due to the smaller effective arm length ($L - t =$ 30 nm) of the "U"-shaped structure than that ($L = 50$ nm) in S-ML shown in Fig. 1b, the effective inductance in the "U"-shaped structure, primarily determined by the total length of the resonant "loop", is smaller than that in S-ML. Thus, based on LC circuit model ($\omega = 1/\sqrt{(LC)}$), a shift to higher resonance frequency (425 THz) is introduced in the "U"-shaped structure, as shown by the red curve in Fig. 4. Second, the effective length of the cut-wire ($P - d + 2t = 160$ nm) is larger than that ($P - d = 120$ nm) in S-ML shown in Fig. 1c. So, it results in a lower resonance frequency (510 THz) of the individual cut-wire than that (540 THz) in S-ML, as shown by the blue curve in Fig. 4 (as all known, the resonance frequency of infinite metal wire is zero when the polarization direction of incident electric field is along the metal wire).

3.3 FOM investigation

The figure of merit (FOM), defined to be $-\mathrm{Re}(n)/\mathrm{Im}(n)$, is analyzed to investigate the loss of S-ML in negative n region. For convenient discussion, two regions are marked in Fig. 2c and d. The apparent difference between them is the value of μ: positive between 397 and 414 THz, negative between 414 and 433 THz. This indicates single negative n and double negative n. According to the difference above, FOM and corresponding transmission are shown in Fig. 5. It can be seen that FOM in double negative region is larger than that in single negative region (for example, FOM ≈ 1 at 420 THz, and FOM ≈ 0.4 at 410 THz). Also, the transmission in the double negative region is about 30% (averaged value), which is much larger than that (10%, averaged value) in the single negative region. This indicates a smaller loss of S-ML in double negative region [22].

4 Parametrical explorations

In this section, we discuss the dependence of the electromagnetic response of S-ML on the parameters of the dielectric grating, including the gradient (θ) and height (h). The results are shown in Fig. 6. It can be seen that θ has little influence on the magnetic resonance at 410 THz when θ bears small variety in Fig. 6a. This result can be understood using LC circuit model. Both the effective inductance and capacitance are not much influenced when θ changes from 90° to 70°, while the electric resonance splits into two resonances.

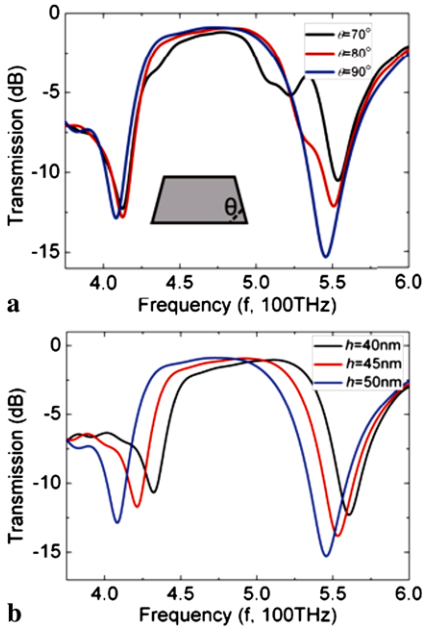

Fig. 6 Transmission spectra (dB) of S-ML with tunable degree (**a**), and height (**b**) of the dielectric grating. The *inset in (a)* shows the cross section of the dielectric grating investigated

In fact, this is caused by the introduction of the parallel component of the side metal layer when θ is not 90°. An apparent trend is that the additional resonance becomes larger and shifts to lower frequency when the parallel component of the side metal layer is larger.

Figure 6b shows the transmission spectra of S-ML with increasing height (h is 40, 45 and 50 nm). First, the magnetic resonance has a red shift when h increases. It is due to the increase of both the effective impedance and capacitance. Second, although the effective length of the oscillator (the metal cut-wire) is not changed, the electric resonance also has a red shift when h increases. Obviously, this is caused by the shift of the magnetic resonance. A simple understanding is that the cut-wire and the "U"-shaped structures are electrically connected in S-ML, and mutual influence exists in electric and magnetic resonances.

5 Conclusions

In summary, a single-layer structure with negative index at visible frequencies is investigated in this paper. Simulation shows that both negative μ and ε are attained at an overlapping range. The structural exploration demonstrates that the simultaneously negative ε and μ is attributed to periodic cut-wire and "U"-shaped structure dissembled from S-ML, respectively. Furthermore, the influences of the gradient and the height of dielectric grating are explored to meet the disfigurements in a practical fabrication process.

Acknowledgements This work was supported by 973 Program of China (No. 2006CB302900) and National Natural Science Foundation of China (No. 60825405).

References

1. J.B. Pendry, A.J. Holden, D.J. Robbins, W.J. Stewart, IEEE Trans. Microw. Theory Tech. **47**, 2075 (1999)
2. T.J. Yen, W.J. Padilla, N. Fang, D.C. Vier, D.R. Smith, J.B. Pendry, D.N. Basov, X. Zhang, Science **303**, 1496 (2004)
3. S. Linden, C. Enkrich, M. Wegener, J. Zhou, T. Koschny, C.M. Soukoulis, Science **306**, 1531 (2004)
4. N. Katsarakis, G. Konstantinidis, A. Kostopoulos, R.S. Penciu, T.F. Gundogdu, M. Kafesaki, E.N. Economou, Th. Koschny, C.M. Soukoulis, Opt. Lett. **30**, 1348 (2005)
5. S. Zhang, W. Fan, B.K. Minhas, A. Frauenglass, K.J. Malloy, S.R.J. Brueck, Phys. Rev. Lett. **94**, 037402 (2005)
6. C. Enkrich, M. Wegener, S. Linden, S. Burger, L. Zschiedrich, F. Schmidt, J.F. Zhou, Th. Koschny, C.M. Soukoulis, Phys. Rev. Lett. **95**, 203901 (2005)
7. G. Dolling, C. Enkrich, M. Wegener, C.M. Soukoulis, S. Linden, Opt. Lett. **30**, 3198 (2005)
8. D.R. Smith, S. Schultz, P. Markos, C.M. Soukoulis, Phys. Rev. B **65**, 195104 (2002)
9. J.B. Pendry, A.J. Holden, W.J. Stewart, I. Youngs, Phys. Rev. Lett. **76**, 4773 (1996)
10. G. Dolling, C. Enkrich, M. Wegener, C.M. Soukoulis, S. Linden, Opt. Lett. **31**, 1800 (2006)
11. S. Zhang, W. Fan, K.J. Malloy, S.R.J. Brueck, N.C. Panoiu, R.M. Osgood, Opt. Express **13**, 4922 (2005)
12. R.A. Shelby, D.R. Smith, S. Schultz, Science **292**, 77 (2001)
13. S. Zhang, W. Fan, N.C. Panoiu, K.J. Malloy, R.M. Osgood, S.R.J. Brueck, Phys. Rev. Lett. **95**, 137404 (2005)
14. V.M. Shalaev, W. Cai, U.K. Chettiar, H.-K. Yuan, A.K. Sarychev, V.P. Drachev, A.V. Kildishev, Opt. Lett. **30**, 3356 (2005)
15. J. Valentine, S. Zhang, T. Zentgraf, E. Ulin-Avila, D.A. Genov, G. Barta, X. Zhang, Nat. Lett. (2008). doi:10.1038
16. G. Dolling, M. Wegener, C.M. Soukoulis, S. Linden, Opt. Lett. **32**, 53 (2007)
17. P.B. Johnson, R.W. Christy, Phys. Rev. B **6**, 4370 (1972)
18. C. Noguez, J. Phys. Chem. C **111**, 3806 (2007)
19. D.R. Smith, S. Schultz, P. Marko, C.M. Soukoulis, Phys. Rev. B **65**, 195104 (2002)
20. X. Chen, T.M. Grzegorczyk, B.-I. Wu, J. Pacheco, J.A. Kong, Phys. Rev. E **70**, 016608 (2004)
21. T. Koschny, P. Markoš, D.R. Smith, C.M. Soukoulis, Phys. Rev. E **68**, 065602(R) (2004)
22. U.K. Chettiar, A.V. Kildishev, H.-K. Yuan, W. Cai, S. Xiao, V.P. Drachev, V.M. Shalaev, Opt. Lett. **32**, 1671 (2007)